

Experimental determination of the hydrothermal solubility of ReS₂ and the Re–ReO₂ buffer assemblage and transport of rhenium under supercritical conditions

Yongliang Xiong^{*a} and Scott A. Wood^{*b}

^aDepartment of Geological Sciences, Rutgers, The State University of New Jersey, 610 Taylor Road, Piscataway, NJ 08854-8066, USA. E-mail: xiongyl@rci.rutgers.edu

^bDepartment of Geological Sciences, University of Idaho, Box 443022, Moscow, ID 83844-3022, USA. E-mail: swood@uidaho.edu

Received 4th October 2001, Accepted 17th December 2001

Published on the Web 11th January 2002

To understand the aqueous species important for transport of rhenium under supercritical conditions, we conducted a series of solubility experiments on the Re–ReO₂ buffer assemblage and ReS₂. In these experiments, pH was buffered by the K–feldspar–muscovite–quartz assemblage; f_{O_2} in sulfur-free systems was buffered by the Re–ReO₂ assemblage; and f_{O_2} and f_{S_2} in sulfur-containing systems were buffered by the magnetite–pyrite–pyrrhotite assemblage. Our experimental studies indicate that the species ReCl₄⁰ is dominant at 400 °C in slightly acidic to near-neutral, and chloride-rich (total chloride concentrations ranging from 0.5 to 1.0 M) environments, and ReCl₃⁺ may predominate at 500 °C in a solution with total chloride concentrations ranging from 0.5 to 1.5 M. The results also demonstrate that the solubility of ReS₂ is about two orders of magnitude less than that of ReO₂. This finding not only suggests that ReS₂ (or a ReS₂ component in molybdenite) is the solubility-controlling phase in sulfur-containing, reducing environments but also implies that a mixing process involving an oxidized, rhenium-containing solution and a solution with reduced sulfur is one of the most effective mechanisms for deposition of rhenium. In analogy with Re, TcS₂ may be the stable Tc-bearing phase in deep geological repositories of radioactive wastes.

Introduction

There has been increasing interest in the aqueous geochemistry of rhenium because of its various important applications as summarized in Xiong and Wood.^{1,2} In our previous publications, the dominant oxidation state of rhenium in high-temperature hydrothermal solutions under geologically reasonable oxygen fugacity conditions was determined experimentally to be +4 by measuring the solubility of ReO₂ as a function of oxygen fugacity.¹ In the temperature range from 100 to 200 °C, Xiong and Wood² suggest that the neutral species, formulated as Re(OH)₄⁰, is important over a wide range of pH, and is responsible for transport of rhenium leading to the enrichment of rhenium in various environments, including sandstone copper deposits and black shales.

In this communication, we present our experimental data on the solubility of rhenium phases under supercritical conditions. The objective of our study is to assess probable rhenium species important under supercritical conditions (up to 510 °C). Based on findings from these experiments, we hope to provide a better understanding of the possible enrichment and deposition mechanisms for rhenium in various high-temperature environments. In particular, our treatment will focus on possible enrichment mechanisms for Re in porphyry copper–molybdenum and skarn molybdenum–(tungsten) deposits. In addition, our experimental results may also provide guidance to applications of the Re–Os system in high-temperature environments.

Methodology

The methodology employed in our experiments under supercritical conditions has been described in detail elsewhere.^{1,3} The

key components of the methodology employed are briefly summarized here.

In our experiments, self-sealing reaction vessels with a volume of approximately 250 mL, lined with gold, and which permit withdrawal of samples at the temperatures and pressures of interest, were used. The pH and f_{O_2} were buffered by thermodynamically well-characterized solid-phase assemblages such as K–feldspar + muscovite + quartz and Re–ReO₂. K–feldspar, quartz, and muscovite were mixed in approximately a 1:1:1 mass ratio and the total mass was approximately 15 g. The source of these solid phases and their respective purities are given in detail elsewhere.^{1,3}

Starting materials were metallic rhenium (99.995%, grain size smaller than 149 µm, minimum grain size ≥ 1.8 µm) and ReO₂ (99.9%, grain size smaller than 44 µm, minimum grain size ≥ 1.8 µm) from Aldrich Chemical Company. The ReS₂ (99%, minimum grain size > 1.8 µm) employed was from Johnson Matthey Company. Magnetite, pyrite and pyrrhotite (research grade) were natural samples and were from Ward's Natural Science Establishment, Inc. Starting materials were loaded in silver or gold capsules as in previous work.¹

After the reaction vessels were assembled into the furnaces, compressed argon was used to check for leaks in the line. Next, the reaction vessels were purged with compressed argon at least three times to dislodge and remove any residual air in the reaction vessels. The vessels were then heated rapidly to the desired temperature and pressure in nichrome resistance furnaces. The amount of electric power provided to the top and bottom of the furnace could be adjusted separately so that the thermal gradient could be controlled precisely. Details of the temperature control and calibration of type K thermocouples used in our experiments can be found in Xiong and Wood.^{1,3} To homogenize the solutions in the vessel, convection was

induced by maintaining the bottom of the vessel 2 °C higher than the top.

Pressure was measured to within ± 10 bar using a pressure transducer and a digital pressure meter from Omega Engineering Company. To minimize the exposure of the transducer to corrosion, the vessel was connected with an Ashcroft Inconel 718 tube analogue gauge in some experimental runs, and the pressure was measured to within ± 15 bar. Both the transducer and Ashcroft analogue gauge were calibrated against a Heise analogue gauge.

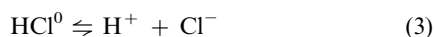
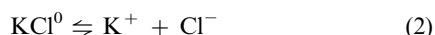
When sampling, supercritical conditions were assured by setting run temperatures and pressures according to the data of Sourirajan and Kennedy⁴ for the analogous NaCl system. Sampling details are similar to those of Xiong and Wood.^{1,3}

The concentrations of Re were determined by inductively coupled plasma-atomic emission spectrometry (ICP-AES) with an axial-view torch (Perkin Elmer Optima 3000 XL). In order to minimize matrix effects, blanks and standard calibration solutions were precisely matched to the samples with respect to matrix. The correlation coefficients of the calibration curves were better than 0.999. The conservative detection limit for rhenium is estimated to be better than 14 ppb [$\sim 7.5 \times 10^{-8}$ mol (kg H₂O)⁻¹] based upon at least three replicate analyses of matrix-matched blanks. The analytical precision in terms of the relative standard deviation (RSD) of replicate analyses is better than 1.5%.

After each run, the starting phases, and the pH and f_{O_2} buffer assemblages were examined by X-ray powder diffraction. No components of the buffers were observed to have been exhausted and no new phases appeared during any run, suggesting that buffered conditions were maintained.

In order to facilitate the interpretation of experimental results, the pH values and molar concentrations of major species in the KCl–H₂O system at different KCl concentrations were calculated according to the following equations using the EQBRM computer code⁵ (Table 1). Equilibrium constants for these reactions were obtained from the SUPCRT92 database⁶ with updated parameters for relevant species for HKF equations from ref. 7–9

Mass-action expressions were:



The charge-balance expression employed was:

$$m_{H^+} + m_{K^+} = m_{Cl^-} + m_{OH^-} \quad (6)$$

And the mass-balance expression was:

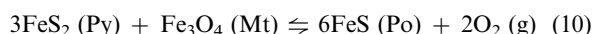
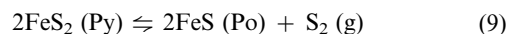
$$m_{\Sigma Cl} = m_{Cl^-} + m_{KCl^0} + m_{HCl^0} \quad (7)$$

Activity coefficients for charged species were calculated using the extended Debye–Hückel equation,¹⁰

$$\log \gamma_i = -AZ_i^2 I^{0.5} / (1 + \hat{a}_i B I^{0.5}) + bI \quad (8)$$

where A and B at 400 °C and 0.5 kbar and 500 °C and 1 kbar are from Helgeson and Kirkham,¹¹ \hat{a} is from the compilation,¹² and b for the similar NaCl system is from Helgeson *et al.*¹³ Activity coefficients of neutral species were assumed to be unity.

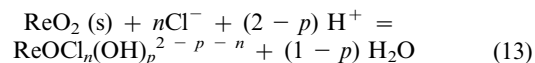
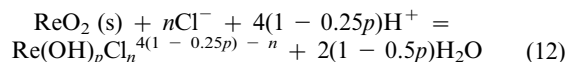
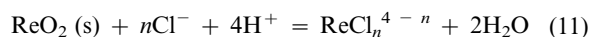
In those experiments assessing the solubility of rhenium sulfide (ReS₂, purity 99.5%, Johnson Matthey Co.) in sulfur-containing environments, f_{O_2} and f_{S_2} were buffered by the magnetite(Mt)–pyrite(Py)–pyrrhotite (Po) assemblage, as shown by the following reactions:



The pH values fixed by the assemblage KMQ in our experiments range from 4.5 to 5.7 at around 400 °C and from 4.6 to 5.7 at around 500 °C, respectively (Table 1) (for reference, neutral pH at 500 °C and 800 bar is ~ 6.0). The pH of the KMQ buffer in a 0.1 mol KCl solution at 500 °C and 550 bar is calculated to be 5.5 (neutral pH at 500 °C and 550 bar is ~ 6.6) and in 0.1 mol KCl solution at 400 °C and 550 bar is calculated to be 5.0 (neutral pH at 400 °C and 550 bar is ~ 5.6), respectively. Therefore, the experiments are all in the near-neutral to slightly acidic pH range.

Experimental design

The purpose of the present experiments was to determine the solubility of rhenium as a function of chloride concentration and pH. As we have demonstrated that, at geologically reasonable oxygen fugacity the dominant oxidation state of rhenium is +4,¹ the general solubility reactions can be expressed as one of the following, the same as those suggested by Xiong and Wood,¹ using ReO₂ as starting material:



Reaction (13) reflects the consideration that some cations with four positive charges such as V⁺⁴ and U⁺⁴ tend to form oxo-aquo-cations before other complexes are formed.¹⁴ Reaction (12) represents the view that there is no structural evidence for cations with four positive charges such as Zr⁺⁴ and Hf⁺⁴ to form “yl” ions like ZrO⁺² and HfO⁺².¹⁵ For simplicity, we follow the convention of Baes and Mesmer¹⁵ for cations with four positive charges. In the present solubility studies, it is not possible to resolve the degree of hydration of the complex or the possible existence of the rhenyl cation (ReO⁺²). Other techniques are needed to resolve these issues in future experimental work.

Using reaction (12) as an example, if the equilibrium constant for reaction (12) is expressed in logarithmic form and rearranged when temperature, pressure, and concentrations of chloride are constant, in log ΣRe versus pH space, the ligand number p for hydroxide can be evaluated according to the slope:

$$(\partial \log \Sigma Re / \partial pH)_{T,P,m_{Cl^-}} = -(4 - p) \quad (14)$$

When temperature, pressure and pH are constant, the ligand number n for chloride can be determined according to the slope in log ΣRe versus log m_{Cl^-} space:

$$(\partial \log \Sigma Re / \partial \log m_{Cl^-})_{T,P,pH} = n \quad (15)$$

The above experimental design has been applied successfully in our experimental work under subcritical conditions.²

Table 1 Rhenium concentrations in equilibrium with various solid-phase assemblages at 400 to 500 °C in KCl solutions ranging from 0.01 to 1.5 mol

Experimental run number	Oxygen fugacity buffer and experimental parameters	Sample number	Run time/h	Concentration from filtered sample/mol (kg H ₂ O) ⁻¹	Concentration from unfiltered sample/mol (kg H ₂ O) ⁻¹
Re-0.01MPP	Mt + Py + Po 0.01 mol KCl 400 °C 550 bar ReS ₂ as starting Material	Re-0.01MPP-1B	28.75	Not available	4.60 × 10 ⁻⁶
		Re-0.01MPP-2B	263.25	9.59 × 10 ⁻⁷	1.09 × 10 ⁻⁶
		Re-0.01MPP-3B	340.5	5.13 × 10 ⁻⁷	6.23 × 10 ⁻⁷
		Re-0.01MPP-4B	455.33	9.47 × 10 ⁻⁷	1.25 × 10 ⁻⁶
		Re-0.01MPP-5B	498	4.99 × 10 ⁻⁷	6.06 × 10 ⁻⁷
		Re-0.01MPP-6B	540.66	4.95 × 10 ⁻⁷	8.04 × 10 ⁻⁷
Re-0.1MPP	Mt + Py + Po 0.1 mol KCl 400 °C 550 bar ReS ₂ as starting Material	Re-0.1MPP-1B	71.25	Not available	3.92 × 10 ⁻⁴
		Re-0.1MPP-2B	189.25	1.57 × 10 ⁻⁶	1.50 × 10 ⁻⁶
		Re-0.1MPP-3B	238.25	6.38 × 10 ⁻⁷	1.26 × 10 ⁻⁶
		Re-0.1MPP-4B	303.75	2.20 × 10 ⁻⁷	8.07 × 10 ⁻⁷
		Re-0.1MPP-5B	405	5.04 × 10 ⁻⁷	9.33 × 10 ⁻⁸
		Re-0.1MPP-6B	467	5.80 × 10 ⁻⁷	2.16 × 10 ⁻⁶
OsO ₂ -0.1RRO	Re-ReO ₂ 0.1 mol KCl 400 °C 550 bar	OsO ₂ -0.1RRO-1B	12	Not available	1.25 × 10 ⁻⁴
		OsO ₂ -0.1RRO-2B	61.75	1.67 × 10 ⁻⁴	1.88 × 10 ⁻⁴
		OsO ₂ -0.1RRO-3B	114.75	2.02 × 10 ⁻⁴	2.27 × 10 ⁻⁴
		OsO ₂ -0.1RRO-4B	179	2.76 × 10 ⁻⁴	3.21 × 10 ⁻⁴
		OsO ₂ -0.1RRO-5B	229.17	3.02 × 10 ⁻⁴	3.22 × 10 ⁻⁴
		OsO ₂ -0.1RRO-6B	276.5	2.86 × 10 ⁻⁴	2.91 × 10 ⁻⁴
		OsO ₂ -0.1RRO-7B	324	2.71 × 10 ⁻⁴	2.88 × 10 ⁻⁴
		OsO ₂ -0.1RRO-8B	394.83	3.16 × 10 ⁻⁴	3.30 × 10 ⁻⁴
Re-0.75/4	Re-ReO ₂ 0.75 mol KCl 400 °C 550 bar	Re-0.75/4-1B	95.5	1.62 × 10 ⁻⁴	1.87 × 10 ⁻⁴
		Re-0.75/4-2B	143.5	1.89 × 10 ⁻⁴	2.07 × 10 ⁻⁴
		Re-0.75/4-3B	190.75	2.02 × 10 ⁻⁴	2.18 × 10 ⁻⁴
		Re-0.75/4-4B	239.75	2.29 × 10 ⁻⁴	2.35 × 10 ⁻⁴
		Re-0.75/4-5B	289.5	1.77 × 10 ⁻⁴	1.94 × 10 ⁻⁴
		Re-0.75/4-6B	330	1.63 × 10 ⁻⁴	1.72 × 10 ⁻⁴
Re-0.5	Re-ReO ₂ 0.5 mol KCl 410 °C 350 bar —	Re-0.5-1B	121	Not available	3.92 × 10 ⁻⁶
		Re-0.5-2B	193	Not available	4.97 × 10 ⁻⁶
		Re-0.5-3B	247	Not available	3.31 × 10 ⁻⁶
		Re-0.5-4B	295	Not available	5.66 × 10 ⁻⁶
		Re-0.5-5B	361	Not available	1.08 × 10 ⁻⁵
		Re-0.5-6B	457	Not available	1.18 × 10 ⁻⁵
		Re-0.5-7B	528.5	Not available	9.22 × 10 ⁻⁶
		Re-0.5-8B	607	Not available	1.36 × 10 ⁻⁵
		Re-0.5-9B	654	Not available	1.43 × 10 ⁻⁵
		Re-0.5-10B	751	Not available	9.54 × 10 ⁻⁶
		Re-0.5-11B	796.5	Not available	1.22 × 10 ⁻⁵
Re-1.0S	Re-ReO ₂ 1.0 mol KCl 410 °C 800 bar Approaching Equilibrium From Lower Temp.	Re-1.0S-1B	143.83	Not available	4.95 × 10 ⁻⁵
		Re-1.0S-2B	233.83	Not available	2.54 × 10 ⁻⁴
		Re-1.0S-3B	333.60	Not available	3.10 × 10 ⁻⁴
		Re-1.0S-4B	410.83	Not available	4.11 × 10 ⁻⁴
		Re-1.0S-5B	488.98	Not available	3.46 × 10 ⁻⁴
		Re-1.0S-6B	538.57	Not available	4.61 × 10 ⁻⁴
		Re-1.0S-7B	679.23	Not available	5.30 × 10 ⁻⁴
		Re-1.0S-8B	732.9	Not available	4.79 × 10 ⁻⁴
		Re-1.0S-9B	795.58	Not available	5.09 × 10 ⁻⁴
		Re-1.0S-10B	846.73	Not available	5.89 × 10 ⁻⁴
		Re-1.0S-11B	942.82	Not available	2.80 × 10 ⁻⁴
		Re-1.0S-12B	990.82	Not available	3.57 × 10 ⁻⁴
		Re-1.0S-13B	1033.82	Not available	5.58 × 10 ⁻⁴
		Re-1.0S-14B	1081.98	Not available	4.56 × 10 ⁻⁴
Re-1.0S	Re-ReO ₂ 1.0 mol KCl 410 °C 800 bar Approaching Equilibrium From Higher temp.	Re-1.0S-15B	64.5	Not available	4.59 × 10 ⁻⁴
		Re-1.0S-16B	136.67	Not available	2.50 × 10 ⁻⁴
		Re-1.0S-17B	236.5	Not available	3.85 × 10 ⁻⁴
		Re-1.0S-18B	303	Not available	2.09 × 10 ⁻⁴
		Re-1.0S-19B	353	Not available	3.59 × 10 ⁻⁴
		Re-1.0S-20B	423.67	Not available	5.62 × 10 ⁻⁴
		Re-1.0S-21B	544	Not available	5.09 × 10 ⁻⁴
		Re-1.0S-22B	616	Not available	5.08 × 10 ⁻⁴
		Re-1.0S-23B	663.5	Not available	4.68 × 10 ⁻⁴
		Re-1.0S-24B	167.5	Not available	5.82 × 10 ⁻⁴
Re-1.0S	1.0 mol KCl 450 °C 800 bar	Re-1.0S-25B	213.17	Not available	5.56 × 10 ⁻⁴
		Re-1.0S-26B	262.5	Not available	5.47 × 10 ⁻⁴
		Re-1.0S-27B	309.5	Not available	4.97 × 10 ⁻⁴
		Re-1.0S-28B	359	Not available	3.78 × 10 ⁻⁴
		Re-1.0S-29B	406.5	Not available	5.44 × 10 ⁻⁴
		Re-1.0S-30B	454	Not available	5.54 × 10 ⁻⁴
		Re-1.0S-31B	526	Not available	5.62 × 10 ⁻⁴
		Re-1.0S-32B	574	Not available	5.06 × 10 ⁻⁴
		Re-1.0S-33B	622	Not available	4.02 × 10 ⁻⁴
		Re-1.0S-34B	670.25	Not available	3.41 × 10 ⁻⁴
		Re-1.0S-35B	718.08	Not available	5.43 × 10 ⁻⁴
		Re-1.0S-36B	722	Not available	7.32 × 10 ⁻⁴

Table 1 Rhenium concentrations in equilibrium with various solid-phase assemblages at 400 to 500 °C in KCl solutions ranging from 0.01 to 1.5 mol (Continued)

Experimental run number	Oxygen fugacity buffer and experimental parameters	Sample number	Run time/h	Concentration from filtered sample/mol (kg H ₂ O) ⁻¹	Concentration from unfiltered sample/mol (kg H ₂ O) ⁻¹
Re-0.5	Re-ReO ₂ 0.5 mol KCl 460 °C 550 bar	Re-0.5-12B	65.3	Not available	2.28 × 10 ⁻⁵
		Re-0.5-13B	143.57	Not available	2.10 × 10 ⁻⁵
		Re-0.5-14B	193.15	Not available	1.54 × 10 ⁻⁵
		Re-0.5-15B	333.82	Not available	8.40 × 10 ⁻⁶
		Re-0.5-16B	388.5	Not available	6.49 × 10 ⁻⁶
		Re-0.5-17B	451.15	Not available	8.60 × 10 ⁻⁶
		Re-0.5-18B	502.32	Not available	9.41 × 10 ⁻⁶
		Re-0.5-19B	598.32	Not available	8.79 × 10 ⁻⁶
		Re-0.5-20B	646.32	Not available	8.57 × 10 ⁻⁶
		Re-0.5-21B	689.32	Not available	6.88 × 10 ⁻⁶
		Re-0.5-22B	737.49	Not available	6.99 × 10 ⁻⁶
Re-0.01RRO	Re-ReO ₂ 0.01 mol KCl 500 °C 550 bar	Re-0.01RRO-1B	5	Not available	1.86 × 10 ⁻⁴
		Re-0.01RRO-2B	9	Not available	3.14 × 10 ⁻⁴
		Re-0.01RRO-3B	47	3.11 × 10 ⁻⁴	3.13 × 10 ⁻⁴
		Re-0.01RRO-4B	94.5	2.91 × 10 ⁻⁴	3.05 × 10 ⁻⁴
		Re-0.01RRO-5B	143.5	2.40 × 10 ⁻⁴	2.41 × 10 ⁻⁴
		Re-0.01RRO-6B	190.5	2.44 × 10 ⁻⁴	2.52 × 10 ⁻⁴
		Re-0.01RRO-7B	238.5	3.27 × 10 ⁻⁴	3.22 × 10 ⁻⁴
Re-0.1RRO	Re-ReO ₂ 0.1 mol KCl 500 °C 550 bar	Re-0.1RRO-1B	52	Not available	5.52 × 10 ⁻⁴
		Re-0.1RRO-2B	69.5	Not available	5.89 × 10 ⁻⁴
		Re-0.1RRO-3B	74.75	Not available	5.63 × 10 ⁻⁴
		Re-0.1RRO-4B	93.5	Not available	6.68 × 10 ⁻⁴
		Re-0.1RRO-5B	211.25	1.24 × 10 ⁻⁴	3.19 × 10 ⁻⁴
		Re-0.1RRO-6B	328	1.89 × 10 ⁻⁴	2.02 × 10 ⁻⁴
		Re-0.1RRO-7B	379.5	7.70 × 10 ⁻⁵	2.05 × 10 ⁻⁴
Re-0.1MPP/2	Mt+Py+Po 0.1 mol KCl 500 °C 550 bar ReS ₂ as starting Material	Re-0.1MPP/2-1B	52.83	Not available	1.18 × 10 ⁻⁵
		Re-0.1MPP/2-2B	70.33	Not available	5.76 × 10 ⁻⁶
		Re-0.1MPP/2-3B	75.58	Not available	3.14 × 10 ⁻⁶
		Re-0.1MPP/2-4B	94.33	7.75 × 10 ⁻⁷	8.44 × 10 ⁻⁷
		Re-0.1MPP/2-5B	212.08	Below detection limit	Below detection limit
Re-0.1MPP/2-6B	328.83	Below detection limit	Below detection limit		
Re/Os-1.0RRO	Re-ReO ₂ 1.0 mol KCl 500 °C 550 bar	Re-1.0RRO-1B	10.5	Not available	1.82 × 10 ⁻⁴
		Re-1.0RRO-2B	99.5	1.83 × 10 ⁻⁴	2.04 × 10 ⁻⁴
		Re-1.0RRO-3B	141.5	1.26 × 10 ⁻⁴	1.51 × 10 ⁻⁴
		Re-1.0RRO-4B	202	1.01 × 10 ⁻⁴	2.07 × 10 ⁻⁴
		Re-1.0RRO-5B	274	2.09 × 10 ⁻⁴	1.94 × 10 ⁻⁴
Re/Os-1.5	Re-ReO ₂ 1.0 mol KCl 500 °C 800 bar	Re/Os-1.5-1B	172	Not available	4.67 × 10 ⁻⁴
		Re/Os-1.5-2B	216.25	Not available	5.49 × 10 ⁻⁴
		Re/Os-1.5-3B	264.67	Not available	8.44 × 10 ⁻⁴
		Re/Os-1.5-4B	314	Not available	1.00 × 10 ⁻³
		Re/Os-1.5-5B	359.67	Not available	1.17 × 10 ⁻³
		Re/Os-1.5-6B	409	Not available	9.02 × 10 ⁻⁴
		Re/Os-1.5-7B	456	Not available	1.07 × 10 ⁻³
		Re/Os-1.5-8B	505.5	Not available	1.36 × 10 ⁻³
		Re/Os-1.5-9B	552	Not available	1.41 × 10 ⁻³
		Re/Os-1.5-10B	599.5	Not available	7.49 × 10 ⁻⁴
		Re/Os-1.5-11B	648.5	Not available	1.30 × 10 ⁻³
		Re/Os-1.5-12B	696.5	Not available	7.18 × 10 ⁻⁴
		Re/Os-1.5-13B	744.5	Not available	7.46 × 10 ⁻⁴
		Re/Os-1.5-14B	792.75	Not available	5.95 × 10 ⁻⁴
		Re/Os-1.5-15B	840.58	Not available	6.93 × 10 ⁻⁴
		Re/Os-1.5-16B	888.41	Not available	5.79 × 10 ⁻⁴
		Re/Os-1.5-17B	913	Not available	1.00 × 10 ⁻³
Re/Os-1.5-18B	937.25	Not available	7.51 × 10 ⁻⁴		
Re-0.5	Re-ReO ₂ 0.5 mol KCl 510 °C 750 bar	Re-0.5-23B	53.5	Not available	2.52 × 10 ⁻⁵
		Re-0.5-24B	122	Not available	8.17 × 10 ⁻⁶
		Re-0.5-25B	169.83	Not available	5.84 × 10 ⁻⁶
		Re-0.5-26B	216.5	Not available	5.25 × 10 ⁻⁶
		Re-0.5-27B	288.67	Not available	8.78 × 10 ⁻⁶
		Re-0.5-28B	388.5	Not available	7.21 × 10 ⁻⁶
		Re-0.5-29B	456	Not available	9.35 × 10 ⁻⁶
		Re-0.5-30B	506	Not available	1.04 × 10 ⁻⁵

Note: Mt—magnetite, Py—pyrite, Po—pyrrhotite.

Experimental results and interpretations

The results of experiments conducted under supercritical conditions are tabulated in Table 1 and plotted in Fig. 1. The molal concentrations of major species in each system as calculated using EQBRM (see above) are listed in Table 2.

From Fig. 1 it is clear that equilibrium was attained after

400 h at 400 °C and 200 h at 500 °C. In comparison, it should be recalled that our experimental results presented elsewhere² under subcritical conditions were buffered with respect to oxygen fugacity and pH by a fixed partial pressure of hydrogen and by aqueous pH buffers, respectively. These buffers equilibrate more quickly than solid assemblages adopted both in the present experiments and those involving platinum

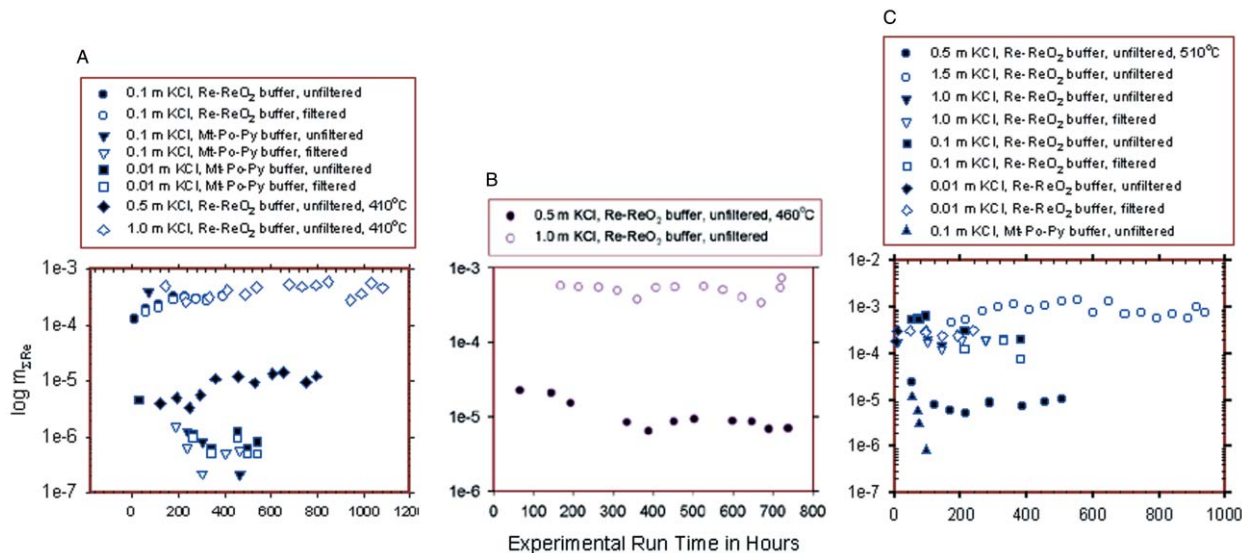


Fig. 1 Rhenium concentration in equilibrium with the K-feldspar-muscovite-quartz and Re-ReO₂ assemblages/ReS₂ in KCl solutions. A Results at 400 °C unless otherwise labeled; B results at 450 °C unless otherwise labeled; and C results at 500 °C unless otherwise labeled.

Table 2 Calculated molal concentrations of major species in the KCl-H₂O system under supercritical conditions

KCl concentration, temperature, and pressure	pH	pOH	log m _{K⁺}	log m _{Cl⁻}	log m _{KCl⁰}	log m _{HCl⁰}	log m _{KOH⁰}
0.01 mol KCl, 400 °C, 550 bar	5.7	5.6	-2.0	-2.0	-3.1	-5.4	-5.3
0.1 mol KCl, 400 °C, 550 bar	5.0	6.3	-1.1	-1.1	-1.7	-4.1	-4.3
0.75 mol KCl, 400 °C, 550 bar	4.5	6.8	-0.23	-0.23	-0.80	-3.2	-5.9
0.5 mol KCl, 410 °C, 550 bar	4.6	6.7	-0.41	-0.41	-0.94	-3.3	-3.2
1.0 mol KCl, 410 °C, 550 bar	4.5	6.8	-0.096	-0.096	-0.71	-3.1	-2.4
1.0 mol KCl, 450 °C, 550 bar	5.0	7.0	-0.067	-0.067	-0.85	-2.8	-0.16
0.5 mol KCl, 460 °C, 550 bar	5.0	6.9	-0.43	-0.43	-0.90	-2.8	-1.4
0.01 mol KCl, 500 °C, 550 bar	5.7	6.2	-2.3	-2.3	-2.4	-4.0	-5.2
0.1 mol KCl, 500 °C, 550 bar	5.2	6.7	-1.5	-1.5	-1.2	-2.8	-4.6
1.0 mol KCl, 500 °C, 800 bar	4.6	7.3	-0.59	-0.59	-0.14	-1.8	-3.0
1.5 mol KCl, 500 °C, 800 bar	4.6	7.3	-0.38	-0.38	0.026	-1.6	-2.5
0.5 mol KCl, 510 °C, 750 bar	4.9	7.2	-1.1	-1.1	-0.39	-2.0	-4.0

group elements (PGE) under supercritical conditions presented elsewhere.³ It can be seen from Fig. 1A and 1C that the concentrations of rhenium in experimental runs using ReS₂ buffered by the Mt-Py-Po assemblage are about two orders of magnitude lower than those using the Re-ReO₂ assemblage at the same temperature and chloride concentration. Experimental results show that there is good agreement of concentrations between filtered and unfiltered samples from experiments involving the Re-ReO₂ assemblage (Fig. 1A-1C), implying

that rhenium is truly in solution. However, there is some scatter between the concentrations from filtered samples and those from unfiltered samples in the experimental run involving ReS₂ buffered by the Mt-Py-Po assemblage (Fig. 1A). This may be due to the fact that experimental runs involving ReS₂ have lower concentrations of rhenium than those using the Re-ReO₂ assemblage, resulting in a larger analytical uncertainty.

The average equilibrium concentrations (\pm two standard deviations) are listed for each experiment in Table 3. All of the

Table 3 Average equilibrium concentrations from experiments under supercritical conditions

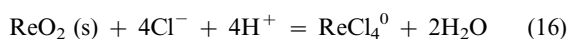
Experimental run number	T / °C	Experimental conditions	Average equilibrium concentration (mol/kg H ₂ O) with 2σ
Re-0.01MPP	400 °C	Mt + Py + Po buffer, 0.01 mol KCl, 550 bar, ReS ₂ as starting material	$7.5 \pm 2.8 \times 10^{-7}$
Re-0.1MPP	400 °C	Mt + Py + Po buffer, 0.1 mol KCl, 550 bar, ReS ₂ as starting material	$1.2 \pm 0.6 \times 10^{-6}$
OsO ₂ -0.1RRO	400 °C	Re-ReO ₂ buffer, 0.1 mol KCl, 550 bar	$3.0 \pm 0.4 \times 10^{-4}$
Re-0.75/4	400 °C	Re-ReO ₂ buffer, 0.75 mol KCl, 550 bar	$1.9 \pm 0.4 \times 10^{-4}$
Re-0.5	410 °C	Re-ReO ₂ buffer, 0.5 mol KCl, 350 bar	$1.2 \pm 0.4 \times 10^{-5}$
Re-1.0S	410 °C	Re-ReO ₂ buffer, 1.0 mol KCl, 800 bar	$5.1 \pm 0.6 \times 10^{-4}$
Re-1.0S	450 °C	Re-ReO ₂ buffer, 1.0 mol KCl, 800 bar	$5.2 \pm 2.2 \times 10^{-4}$
Re-0.5	460 °C	Re-ReO ₂ buffer, 0.5 mol KCl, 550 bar	$8.0 \pm 2.0 \times 10^{-6}$
Re-0.01RRO	500 °C	Re-ReO ₂ buffer, 0.01 mol KCl, 550 bar	$2.9 \pm 0.6 \times 10^{-4}$
Re-0.1RRO	500 °C	Re-ReO ₂ buffer, 0.1 mol KCl, 550 bar	$2.1 \pm 1.1 \times 10^{-4}$
Re-0.1MPP/2	500 °C	Mt + Py + Po buffer, 0.1 mol KCl, 550 bar, ReS ₂ as starting material	$3.2 \pm 2.0 \times 10^{-6}$
Re/Os-1.0RRO	500 °C	Re-ReO ₂ buffer, 1.0 mol KCl, 550 bar	$2.0 \pm 0.1 \times 10^{-4}$
Re/Os-1.5	500 °C	Re-ReO ₂ buffer, 1.5 mol KCl, 800 bar	$9.1 \pm 2.0 \times 10^{-4}$
Re-0.5	510 °C	Re-ReO ₂ buffer, 0.5 mol KCl, 750 bar	$8.2 \pm 3.6 \times 10^{-6}$

data after 200 h and 400 h are included in the calculation of the average equilibrium concentrations at 500 and 400 °C, respectively.

Interpretation of data. From Table 3, it is apparent that at similar chloride concentrations and pH, the rhenium concentrations from experiments using ReS₂ are about two orders of magnitude lower than those from experiments using the Re–ReO₂ buffer assemblage. This suggests that ReS₂ (or the ReS₂ component in molybdenite or other sulfides) is a solubility-controlling phase in high-temperature environments containing sulfur.

Ideally, the chloride- and pH-dependence of the solubility of rhenium is independently evaluated according to eqn. (11) and (12), as we did under subcritical conditions.² However, because the KMQ buffer was adopted in our experiments under supercritical conditions, pH and chloride dependence cannot be evaluated independently; *i.e.*, the coefficient *p* in reaction (12) cannot be evaluated by keeping chloride concentration constant while pH is changed independently. In this communication, we assumed that mixed chloride complexes with hydroxyl suggested in reaction (12) or (13) are not important in the present experiments considering the conditions of the high temperatures, relatively high concentration of chloride, and slightly acidic to near-neutral pHs. This assumption is mainly based on the findings of previous studies which demonstrated increased stability of chloride complexes, simplified speciation, and the unimportance of mixed complexes at high temperatures (*i.e.*, 500 °C).^{16,17} Therefore, the interpretation of chloride dependence is based on reaction (11). However, it should be cautioned that this assumption is subject to experimental verification in the future.

To evaluate the chloride-dependence of the solubility of the assemblage Re–ReO₂, log *m*_{ΣRe} is plotted *versus* log *m*_{Cl⁻} at constant pH in accordance with eqn. (15). For this purpose, the rhenium concentration data from Re–0.5, Re–0.75/4 and Re–1.0S (Table 3) are plotted against log *m*_{Cl⁻} (Fig. 2). Note that the pH is almost constant (from 4.5 to 4.6) in these experimental runs (Table 1), but the measured Re concentrations were corrected for pH differences assuming the pH-dependence indicated by reaction (11). As the slope of a straight line fit to the data in Fig. 2 is close to 4 (3.94 ± 0.35 , $R^2 = 0.99$), the dominant species appears to be ReCl₄⁰ according to reaction (16):



It is also possible that small amounts of ReCl₃⁺ and ReCl₅⁻ are present in addition to ReCl₄⁰, or less likely, that

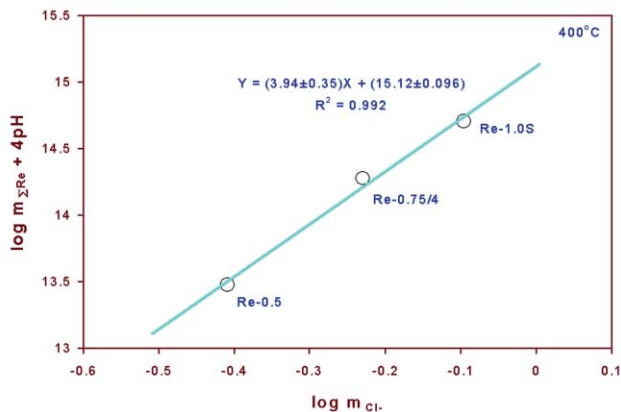


Fig. 2 Plot of logarithmic rhenium concentration (corrected for pH variations) *versus* logarithmic chloride concentration at 400 °C. Only experimental runs involving Re–ReO₂ assemblage were considered and pH was almost constant in these runs.

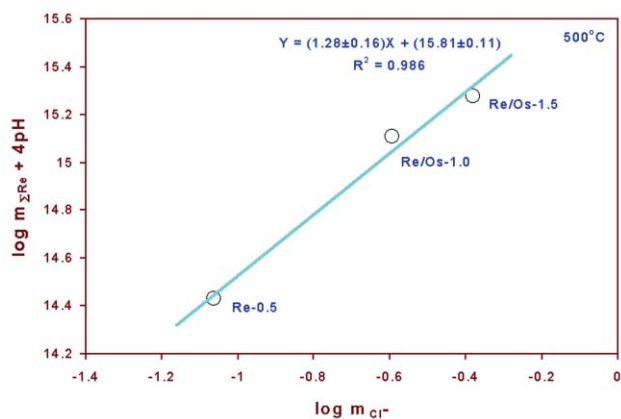


Fig. 3 Plot of logarithmic rhenium concentration (corrected for pH) *versus* logarithmic chloride concentration for solutions in equilibrium with Re and ReO₂ at 500 °C.

approximately equal proportions of ReCl₃⁺ and ReCl₅⁻ are present instead of ReCl₄⁰.

It should be mentioned that we attach considerable uncertainty to the interpretation of the chloride dependence of the experimental data at 500 °C because the variation in pH is 0.3 log units for these experiments. The solubility correction introduced by such pH differences should be more than one log unit according to reaction (11), which may result in large uncertainties in the chloride ligand number when determined as described in the preceding paragraph. The slope determined with the pH correction according to reaction (11) is 1.28 ± 0.16 ($R^2 = 0.985$) (Fig. 3), whereas the slope determined without the pH correction is 2.99 ± 0.016 ($R^2 = 0.99997$) (Fig. 4). Judging from the results at 400 °C and at lower temperatures,² a slope of ~ 3 (corresponding to ReCl₃⁺) is more likely than a slope of ~ 1 (corresponding to ReCl⁺³) at 500 °C. This interpretation is also supported by the relatively small variation of calculated equilibrium constants as a function of ionic strength (see below). However, as the pH differences are relatively large in these experiments, more experiments are certainly needed to refine the interpretations at 500 °C.

It is of interest to note that there is a negative dependence on temperature in the temperature range from 400 to 500 °C in the same solution, implying that there is a retrograde solubility of the Re–ReO₂ buffer assemblage. This can be demonstrated by examining the results from OsO₂–0.1RRO at 400 °C and Re–0.1RRO at 500 °C. The former has an average equilibrium concentration of $3.0 \pm 0.4 \times 10^{-4}$ molal, whereas the latter has an average equilibrium concentration of $2.1 \pm 1.1 \times 10^{-4}$ molal. This trend is also suggested by the Re–0.5 runs at 410

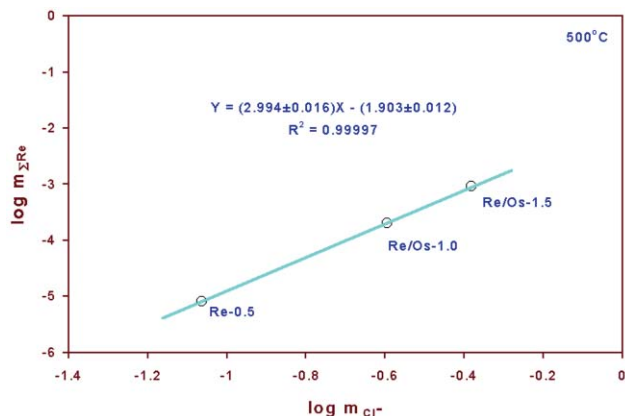
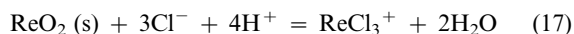


Fig. 4 Plot of logarithmic rhenium concentration (without pH corrections) *versus* logarithmic chloride concentration for solutions in equilibrium with Re and ReO₂ at 500 °C.

and 510 °C, and by the Re-1.0S run (1.0 mol KCl) at 410 °C and the Re/Os-1.0RRO run (1.0 mol KCl) at 500 °C. In addition to higher calculated pH at 500 than at 400 °C, this may be due to the combination of decreasing free chloride concentration with decreasing chloride ligand number with temperature. For example, in a 1.0 mol KCl solution, the concentration of free chloride decreases from about -0.096 log units at 410 °C to about -0.59 log units at 500 °C (Table 1), *i.e.*, a decrease of ~0.6 log units. This decrease in the concentration of free chloride with increasing temperature may also be responsible for the apparent decrease in chloride ligand number as temperature increases from 400 to 500 °C (see the preceding paragraph). On the other hand, the solubility of ReS₂ shows a slight increase in solubility between 400 and 500 °C (*cf.*, Re-0.1MPP at 400 °C and Re-0.1MPP/2 at 500 °C).

Derivation of equilibrium constants. In order to calculate thermodynamic equilibrium constants according to reaction (16), the activity coefficient of the neutral species, ReCl₄⁰, is assumed to be unity. As mentioned before, the activities of other species were calculated by using the extended Debye-Hückel equation and EQBRM code. The thermodynamic equilibrium constants for reaction (16) at 400 °C at different ionic strengths are listed in Table 4. At 500 °C, the species ReCl₃⁺ was identified tentatively as the predominant species. The thermodynamic equilibrium constant for reaction (17) at 500 °C



was estimated. In these calculations, the extended Debye-Hückel equation¹⁰ is used to estimate the activity coefficient for ReCl₃⁺; \hat{a} is assumed to be the same as other +4-charged ions, and is taken from the compilation.¹² It is apparent from Table 4 that there is relatively little variation in the calculated thermodynamic equilibrium constants for both reactions (16) and (17) as a function of ionic strength, lending support to our assignment of the stoichiometry of the Re-chloride complexes.

Implications

The above results indicate that, in high-temperature environments, appreciable amounts of rhenium can be dissolved in chloride-containing (log m_{Cl^-} = -0.4 to -0.1) aqueous fluids as the neutral chloride species, ReCl₄⁰. It is also of importance to note that ReS₂ is much less soluble than ReO₂ (about two orders of magnitude lower). These conclusions have bearing on the transport and deposition of rhenium in various environments and our data are the first step in the quantitative elucidation of origins of rhenium deposits in these environments. In the following, we apply our results to various environments and explore their implications.

As mentioned above, the solubility of ReS₂ is about two orders of magnitude lower than that of ReO₂. This has important implications. First of all, it is apparent that rhenium will be stabilized as a sulfide phase(s) in environments where reduced sulfur is present. This explains why rhenium sulfides occur in a

wide range of environments including mafic and ultramafic complexes such as the Stillwater Complex¹⁸ and fumarolic deposits from volcanoes,¹⁹ whereas sulfur-free rhenium phases have limited occurrences. Second, it can be inferred that samples which have been subject to alteration by oxidizing fluids are likely to have experienced rhenium remobilization, and therefore they are not good candidates for Re-Os radiogenic investigations. Third, it can be deduced that reducing fluids containing sulfur have much less capacity for transporting rhenium, and therefore environments dominated by reducing fluids are not favorable to formation of rhenium deposits of importance. To form rhenium deposits of significance, oxidizing fluids must be operative at some stage(s) of ore formation. On the other hand, reducing fluids have the least ability to disturb the Re-Os system. In the following, transport of rhenium by hydrothermal fluids is addressed quantitatively.

Quantitative assessment of potential size of rhenium mineralization in porphyry copper-molybdenum and skarn tungsten-molybdenum systems

Molybdenite in porphyry copper-molybdenum and skarn tungsten-molybdenum systems has been observed to be enriched in Re.²⁰⁻²⁸ It is of special interest to note that existing reserves of rhenium indicate that porphyry copper-molybdenum systems are very important.²³ In the following, we first present field observations on rhenium mineralization in skarn tungsten-molybdenum and porphyry copper-molybdenum systems and then compare these observations with our quantitative predictions based on our experimental data.

Field observations: The Little Boulder Creek skarn molybdenum deposit in Idaho can be used as an example to estimate the size of skarn Mo-(W) systems and the amount of rhenium mineralization. The reserves of ores with a grade of 0.15 wt% of MoS₂ are 167 million tons.²⁹ Although the rhenium concentration in molybdenite in this deposit is not available, we may assume that the rhenium concentration in molybdenite in this deposit is similar to the rhenium concentration in other skarn Mo-(W) deposits. For example, Stein *et al.*²⁹ determined that the rhenium concentration in molybdenite in the Schwartz, Klee and Meyer skarn Mo-W deposits in the Pitkaranta district, Russia, ranges from 130 to 479 ppm with an average of 224 ppm. Assuming the rhenium concentration in molybdenite in the Little Boulder Creek deposit is of the order of 100 to 200 ppm, the mass of rhenium in this deposit is estimated to be from ~2.5 × 10⁷ to ~5 × 10⁷ grams (Table 5).

In the El Teniente porphyry Cu-Mo mine, the grade of rhenium in ores is 10 ppm (10 grams tonne⁻¹).²³ As ore reserves are estimated to be about 3.5 billion tonnes, the total mass of rhenium in the ore reserves is about 3.5 × 10¹⁰ grams.²³ In addition, this deposit has about 4 × 10⁸ tonnes of tailings in its waste dumps with a grade of 9 grams tonne⁻¹ of rhenium.²³ Therefore, the total rhenium in this deposit is ~4 × 10¹⁰ grams (Table 5).

Predictions: In order to determine, from our experimental solubility data, the total amount of Re that can be transported in porphyry Cu-Mo and skarn Mo-W deposit-forming systems, the total amount of fluid involved in these systems

Table 4 Derived thermodynamic equilibrium constants at 400 and 500 °C

Reaction	Temperature	Experimental run	Ionic strength	log K
ReO ₂ (s) + 4Cl ⁻ + 4H ⁺ = ReCl ₄ ⁰ + 2H ₂ O	400 °C	Re-0.5	0.39	17.96
		Re-0.75/4	0.59	18.48
		Re-1.0S	0.80	18.73
		Average		18.39 ± 0.64 (2σ)
ReO ₂ (s) + 3Cl ⁻ + 4H ⁺ + H ₂ O = ReCl ₃ ⁺ + 2H ₂ O	500 °C	Re-0.5	0.086	18.69
		Re/Os-1.0RRO	0.25	18.26
		Re/Os-1.5	0.42	18.62
		Average		18.52 ± 0.47 (2σ)

Table 5 Predictions and field observations of potential size of rhenium mineralization in porphyry copper–molybdenum and Skarn tungsten–molybdenum systems

Predictions and field observations	T/°C	Solubility controlling phase	log ₁₀ a _{SiO₂}	log ₁₀ f _{O₂}	pH	log a _{Cl⁻}	Log a _{Σ,S}	Transportable re assuming saturation with solid phase in grams	Remarks and references for thermodynamic parameters
This study	400 to 500	ReS ₂	-26.9 to -21.6	-7.6 to -4.8	5.0, KMQ to 5.2, KMQ	-1.5 to -2.3	-1.2 to 0	Typical porphyry Cu–Mo systems: ~2 × 10 ⁸ to ~6 × 10 ⁸ (~2 × 10 ¹⁰ to ~6 × 10 ¹⁰ for giant porphyry Cu–Mo systems)	Log f _{O₂} , log f _{S₂} , and log a _{SS} are calculated from MPP buffer ^d
Porphyry copper–molybdenum system	350 to 550	Solid solution of ReS ₂ and MoS ₂	-26.5 to -16.5 ^e	PP buffer ^b	KMQ buffer ^c	-1.0	-1.0	Skarn W–Mo systems: ~4 × 10 ⁷ to ~1.2 × 10 ⁸ (El Teniente, giant porphyry Cu–Mo)	ref. 40
Skarn tungsten–molybdenum system	400 to 650	Solid solution of ReS ₂ and MoS ₂	-24.1 to -22.1	-8.2 to -6.25	KMQ and WQ buffers ^c	0.17 to > 1.4 (log m _{NaCl}) ^f	~ -0.4 ^g	~8 × 10 ⁶ (La Disputada, typical porphyry Cu–Mo)	ref. 32

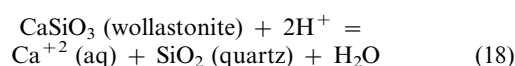
^aMagnetite–hematite buffer. ^bPP: pyrite–pyrrhotite buffer. ^cKMQ: K–feldspar–muscovite–quartz buffer. ^dMPP: magnetite–pyrite–pyrrhotite buffer. ^eWQ: wollastonite–quartz buffer, which should buffer pH values in near-neutral range as mentioned in the text. ^fConverted from salinity ranging from >60 wt% NaCl eq. to ~8 wt% NaCl eq. ^gAs log m_{FeSO₄}, King Island.

must be estimated. The total amount of Re predicted based on our experimental results can then be compared to the amounts calculated in the preceding section from grade and tonnage data.

The amount of fluid involved in a typical porphyry Cu–(Mo) system has been estimated to be ~10¹⁵ grams using the average tonnage of copper (~1 million tonnes) and the copper concentrations in ore-forming fluids (1000 ppm).³ In giant porphyry Cu–Mo systems such as El Teniente porphyry Cu–Mo mine, the total mass of fluid involved may be one to two orders of magnitude higher than that in a typical porphyry Cu–Mo system. For example, the tonnage of copper in El Teniente porphyry Cu–Mo mine is at least 31.5 million tonnes.²⁴ Therefore, a total mass of fluids of ~10¹⁷ grams may be reasonable. The pH of porphyry Cu–(Mo) systems is likely to be buffered by the KMQ assemblage.³ Other thermodynamic parameters in porphyry Cu–(Mo) systems employed in the present predictions have been described in Xiong and Wood.³

In order to estimate the total mass of fluids involved in the formation of a typical skarn tungsten–molybdenum system, the calculated scheelite solubility (39 ppm) in 1.0 mol NaCl solution at 600 °C and 2000 bar of Wood and Samson³¹ is used. This calculated value has been demonstrated to be in excellent agreement with an experimentally measured value.³¹ The Molyhill skarn W–Mo deposit in the Northwestern Territory, Australia, has reserves of 1.5 million tons of ores with a WO₃ grade of 1.0 wt%.³² Apparently, the mass of tungsten in the Molyhill deposit is 1.2 × 10¹⁰ grams. The total mass of fluid involved should be ~3.0 × 10¹⁴ grams according to the solubility of scheelite cited above, assuming that all the tungsten in the fluid is deposited. The Osgood Mountains W–Mo skarns in Humboldt County, Nevada, USA, has reserves of 1.4 million tons of ores with a WO₃ grade of 0.45 wt%.³² The mass of tungsten in this deposit is 5 × 10⁹ grams. Therefore, the estimated total mass of fluid involved should be ~1.3 × 10¹⁴ grams. Consequently, based on the estimated total mass of fluids involved in these two deposits, we assume that the total mass of fluid involved in the formation of a typical W–Mo skarn system should be in the neighborhood of ~2 × 10¹⁴ grams.

The pH of skarn W–Mo systems is likely to be buffered by various assemblages such as the wollastonite–quartz assemblage, which is common in the distal zone of W–Mo skarns:



Although the wollastonite–quartz assemblage has not been deliberately calibrated as a pH buffer, it has been reasoned that this assemblage should buffer pH values in the near-neutral range,³³ which is close to our experimental pH values. In the endoskarn zone, where major W–Sn mineralization occurs, the pH of initial mineralizing fluids exsolved from crystallizing (granitoid) magmas should be buffered by mineral assemblages of granitoid rocks such as quartz + K–feldspar + muscovite. For example, in the endoskarn of the Sangdong deposit, Korea, biotite skarn and muscovite skarn are dominant.³² As the quartz + K–feldspar + muscovite assemblage was employed as a pH buffer in our experiments, the pH values in our experiments should be most likely to resemble those in the early stages of mineralizing fluids.

It has been documented that fluids responsible for proximal skarns with which W–Mo mineralization is generally associated have salinities ranging from >60 wt% NaCl eq. to ~8 wt% NaCl eq.,³² which correspond to concentrations of NaCl ranging from ~1.5 M to higher than ~26 M. Fluids responsible for distal skarns commonly have lower salinities ranging from ~12.5 to ~1.25 wt% NaCl eq.,³² corresponding to concentrations of NaCl from ~0.2 to ~2.5 M. Obviously,

these salinities, especially those in fluids responsible for proximal skarns, are generally higher than those in our experiments. In this respect, our solubility data yield minimum estimates of the amount of Re that can be transported by these hydrothermal systems (but see comments below regarding the occurrence of ReS₂ in solid solution).

Assuming the solubility-controlling phase is pure ReS₂ and using the estimated total masses of fluids in typical porphyry Cu–(Mo) and skarn W–Mo systems mentioned above, when we apply our solubility data solutions with total chloride concentration of 0.1 M (Table 3) at 400 °C (1.2×10^{-6} mol kg⁻¹ H₂O) and at 500 °C (3.2×10^{-6} mol kg⁻¹ H₂O) to the above systems, the rhenium that can be transported by typical porphyry Cu–Mo and skarn W–Mo systems ranges from $\sim 2 \times 10^8$ to $\sim 6 \times 10^8$ and from $\sim 4 \times 10^7$ to $\sim 1.2 \times 10^8$ grams, respectively (Table 5). It should be emphasized that the experimental conditions are comparable to those conditions prevailing in porphyry Cu–Mo and skarn W–Mo systems (Table 5), except that the salinities in our experiments are somewhat lower. Therefore, direct application of our experimental results using ReS₂ as the starting material and magnetite–pyrite–pyrrhotite assemblage to buffer f_{O_2} and f_{S_2} is well justified. However, the ReS₂ used in our experiments is a pure end-member. In the natural systems, it is likely that a solid solution between MoS₂ and ReS₂ would control the solubility of rhenium as suggested in Table 5. It is well known that the solubility of a component in solid solution is generally less than that of the pure end-member phase because the activity of the solid solution is less than unity.³⁴ Although the concentrations of rhenium in molybdenite (MoS₂) have been determined in several deposits as mentioned above, the activity coefficients of ReS₂ in MoS₂–ReS₂ solid solution system are not known. Therefore, the activity of ReS₂ in such solid solutions cannot be quantitatively evaluated at present. However, it can be expected that pure ReS₂ should have higher solubility than the solid solution between MoS₂ and ReS₂. Notice that our predicted tonnage of rhenium mineralization for skarn W–Mo systems is on the same order of magnitude as the observed tonnage in a typical skarn W–Mo systems (Table 5). Our predicted tonnage of rhenium mineralization for porphyry Cu–Mo systems is about one order of magnitude higher than the observed tonnage in typical porphyry systems (such as La Disputada, Chile), but is on the same order of magnitude as the tonnage observed in the giant porphyry Cu–Mo systems (e.g., El Teniente, Chile) (Table 5). Therefore, when the fact that solid solution of MoS₂ and ReS₂ controls solubility is taken into account, our experimental results are in excellent agreement with field observations and our results for giant porphyry Cu–Mo systems (Table 5) predict that the El Teniente deposit-forming fluid was probably close to saturation with the ReS₂ component in solid solution with molybdenite.

In the Chenmanshan skarn and porphyry deposit (where molybdenite is observed) in Juijiang, Jiangxi Province, China, the grade of rhenium is $6 \times 10^{-5}\%$.³⁵ The reserves of Cu in this deposit were 2.1×10^6 tons³⁶ and the grade of Cu was 0.75%.³⁵ Therefore, the total amount of ore is estimated to be $\sim 2.8 \times 10^{14}$ grams. Hence, the amount of Re that had been transported is computed to be $\sim 10^8$ grams. In comparison with the above minimum mass of Re that can be transported ($\sim 2 \times 10^8$ to $\sim 6 \times 10^8$ grams) in a typical porphyry system, the Chenmanshan porphyry deposit-forming fluid may have also been saturated with ReS₂ or its solid solution with other sulfides.

Deposition of rhenium

As the stabilities of the predominant rhenium complexes deduced from our experiments, i.e., ReCl₄⁰ and ReCl₃⁺, have strong dependences on chloride concentration, we can infer that dilution owing to mixing of high-concentration chloride fluids with low-chloride fluids is one of most effective

mechanisms for the deposition of rhenium from porphyry systems. It also needs to be realized that, according to reactions (16), (17), (19) and (20)



the solubility of ReO₂ or ReS₂ should decrease strongly with increasing pH. Therefore, an increase in pH could induce precipitation of rhenium in chloride-rich fluids. However, hydroxy complexes of rhenium may become important at higher pH ranges in chloride-poor fluids, in which case an increase in pH might possibly cause an increase in rhenium solubility. In addition, from the fact that ReS₂ has much lower solubility than Re or ReO₂, we can conclude that mixing processes involving an oxidizing fluid transporting rhenium and a fluid containing reduced sulfur should be an effective depositional mechanism for rhenium.

The slight prograde solubility of ReS₂ in the temperature range from 400 to 500 °C means that more rhenium sulfide is dissolved at higher temperatures. This is different from the Re–ReO₂ assemblage in sulfur-free environments, which shows a slight retrograde solubility in the temperature range from 400 to 510 °C. The slight prograde solubility of ReS₂ might explain the puzzling observation that molybdenite deposited at higher temperatures has lower rhenium concentration (i.e., lower content of ReS₂).^{20,37} This explanation is contingent upon a weak or retrograde temperature dependence of molybdenite solubility over the above temperature range. However, regarding the solubility of molybdenite in hydrothermal solutions, a consistent picture has not emerged.³⁸

The much lower solubility of ReS₂ compared to that of the Re–ReO₂ assemblage also has implications to disposal of fissionogenic ⁹⁹Tc, for which Re is a good analogue.³⁹ As ReS₂ is the stable phase in most subsurface geological environments, TcS₂ should be the preferred phase in deep geological repositories for radioactive wastes. This can ensure that even if radioactive wastes in deep geological repositories interact with solution at elevated temperatures in the worst-case scenario, release of ⁹⁹Tc would be at a minimum. To achieve this goal, radioactive wastes containing ⁹⁹Tc should be sequestered as TcS₂.

Acknowledgement

Research grants from the National Science Foundation (EAR-9614773) to S.A.W. and from the Geological Society of America to Y.-L.X. are gratefully acknowledged. This paper benefitted from the constructive reviews of two referees for *Geochemical Transactions*, which significantly improved our presentation. Thanks are extended to Dr Martin Schoonen, the editor of this special collection of papers honoring Dr Hubert Barnes, for handling our manuscript. We would also like to take this opportunity to express our appreciation of Dr Hubert Barnes, one of the founders of experimental hydrothermal geochemistry, for the tremendous impact he and his colleagues have had on the field of hydrothermal geochemistry.

References

- 1 Y.-L. Xiong and S. A. Wood, *Chem. Geol.*, 1999, **158**, 245.
- 2 Y.-L. Xiong and S. A. Wood, *Econ. Geol.*, 2001, **96**, 1429.
- 3 Y.-L. Xiong and S. A. Wood, *Mineral. Petrol.*, 2000, **68**, 1.
- 4 S. Sourirajan and G. C. Kennedy, *Am. J. Sci.*, 1962, **260**, 115.
- 5 G. M. Anderson and D. A. Crerar, *Thermodynamics in Geochemistry*, Oxford University Press, New York, 1993, p. 588.
- 6 J. W. Johnson, E. H. Oelkers and H. C. Helgeson, *Comput. Geosci.*, 1992, **18**, 899.
- 7 D. A. Sverjensky, J. J. Hemley and W. M. D'Angelo, *Geochim. Cosmochim. Acta*, 1991, **55**, 989.

- 8 V. A. Pokrovskii and H. C. Helgeson, *Geochim. Cosmochim. Acta*, 1997, **61**, 2175.
- 9 B. R. Tagirov, A. V. Zotov and N. N. Akinfiev, *Geochim. Cosmochim. Acta*, 1997, **61**, 4267.
- 10 R. W. Henley, A. H. Truesdell, P. B. Barton Jr. and J. A. Whitney, *Fluid—mineral Equilibria in Hydrothermal Systems, Reviews in Economic Geology Volume 1*, The Economic Geology Publishing Company, El Paso, Texas, 1984, p. 267.
- 11 H. C. Helgeson and D. H. Kirkham, *Am. J. Sci.*, 1974, **274**, 1199.
- 12 D. K. Nordstrom and J. L. Munoz, *Geochemical Thermodynamics*, Blackwell Scientific Publications, Boston, 1986, pp. 477.
- 13 H. C. Helgeson, D. H. Kirkham and G. C. Flowers, *Am. J. Sci.*, 1981, **281**, 1249.
- 14 J. Burgess, *Metal ions in solution*, Ellis Horwood Limited, Chichester, UK, 1978, p. 481.
- 15 C. F. Baes Jr. and R. E. Mesmer, *The Hydrolysis of Cations*, John Wiley and Sons, New York, 1976, p. 489.
- 16 S. A. Wood, D. A. Crerar and M. P. Borcsik, *Econ. Geol.*, 1987, **82**, 1864.
- 17 G. H. Brimhall and D. A. Crerar, in *Thermodynamic Modeling of Geological Materials: Minerals, Fluids and Melts, Reviews in Mineralogy, Volume 17*, ed. I. S. E. Carmichael and H. P. Eugster, 1987, p. 235.
- 18 M. Tarkian, R. M. Housley and A. Volborth, *Eur. J. Mineral.*, 1991, **3**, 977.
- 19 M. A. Korzhinsky, S. Tkachenko, K. I. Shmulovich, Y. A. Taran and G. S. Steinberg, *Nature*, 1994, **369**, 51.
- 20 M. Fleischer, *Econ. Geol.*, 1959, **54**, 1406.
- 21 L. Paganelli, *Geochim. Cosmochim. Acta*, 1963, **27**, 401.
- 22 G. H. Ripley, *Geochim. Cosmochim. Acta*, 1967, **31**, 1489.
- 23 A. Sutulov, *Molybdenum and rhenium recovery from porphyry coppers*. University of Concepcion, Chile, 1970, p. 259.
- 24 A. Sutulov, *Copper porphyries*. University of Concepcion, Chile, 1975, p. 206.
- 25 Y. M. Poplavko, F. F. D'yakonova and L. V. Mel'nikova, *Geochem. Int.*, 1984, **21(2)**, 40.
- 26 D. Huang, Y. Wang and F. Nie, *Chin. J. Geochem.*, 1988, **7(2)**, 136.
- 27 T. E. McCandless, J. Ruiz and A. R. Campbell, *Geochim. Cosmochim. Acta*, 1993, **57**, 889.
- 28 H. J. Stein, R. J. Markey, J. W. Morgan, A. Du and Y. Sun, *Econ. Geol.*, 1997, **92**, 827.
- 29 L. D. Meinert, *Geosci. Can.*, 1992, **19**, 145.
- 30 H. J. Stein, R. J. Markey, J. W. Morgan, K. Sundblad and A. Larin, in *The seventh international symposium on Rapakivi granites and related rocks*, ed. I. Haapala, O. T. Ramo and P. Kosunen, abstract volume, 1996, p. 68.
- 31 S. A. Wood and I. M. Samson, *Econ. Geol.*, 2000, **95**, 143.
- 32 T. A. P. Kwak, *W-Sn Skarn Deposits and Related Metamorphic Skarns and Granitoids*, Elsevier Science Publishers B. V., Amsterdam, The Netherlands, 1987, p. 451.
- 33 Z.-X. Xie and J. V. Walther, *Geochim. Cosmochim. Acta*, 1993, **57**, 1947.
- 34 W. Stumm and J. J. Morgan, *Aquatic Chemistry*, John Wiley and Sons, Inc., New York, 1970, p. 583.
- 35 Y.-F. Chang, X.-P. Liu and Y.-C. Wu, *The copper-iron belt of the middle and lower reaches of the Yangtse River (Changjian River)*, Geological Publishing House, Beijing, **1991**, 379.
- 36 Y.-S. Zhai, Y.-L. Xiong, S.-Z. Yao and X.-D. Lin, *Ore Geol. Rev.*, 1996, **11**, 229.
- 37 D. L. Giles and J. H. Schilling, 24th International Geological Congress, Montreal, Section 10, 1972, p. 145.
- 38 S. A. Wood and I. M. Samson, in *Techniques in Hydrothermal Ore Deposits: Reviews in Economic Geology*, ed. J. Richards and P. Larson, 1998, **v. 10**, p. 33–80.
- 39 D. G. Brookins, *Appl. Geochem.*, 1986, **1**, 513.
- 40 D. A. Crerar and H. L. Barnes, *Econ. Geol.*, 1976, **71**, 772.